

579

Supplemental Information for

580

“Predicting evolutionary rescue via evolving plasticity in stochastic environments”

581

Jaime Ashander, Luis-Miguel Chevin, Marissa L. Baskett

582

Proceedings of the Royal Society B

583

<http://dx.doi.org/10.1098/rspb.2016.1690>

584 **Appendix A. Approximate dynamics of growth rate in terms of maladaptation $x(t)$**

585 Our equation (2) shows the Malthusian growth rate $r(t)$ is the sum of the maximum Malthusian growth
 586 rate r_{\max} , the variance load L_G , and the lag load L_L with $r_{\max} = \log W_{\max}$, $L_G = \log \left(\sqrt{S(\varepsilon_c(t))\omega^2} \right)$,
 587 and $L_L = \frac{S(\varepsilon_c(t))}{2}x(t)^2$,

$$\log \bar{W}(t) = r_{\max} + L_G(t) + L_L(t). \quad (\text{A.1})$$

588 Below, we derive an approximation to this where the only time dependence is through the squared
 589 maladaptation $x(t)^2 = (\bar{z}(t) - \theta(\varepsilon_s(t)))^2$.

590 *Appendix A.1. Strength of selection*

591 The strength of selection, $S(\varepsilon_c(t))$, appears in both the variance load L_G and lag load L_L but depends
 592 inversely on the phenotypic variance, which changes due to stochastic variation in the environmental
 593 cue, which affects the phenotype. Therefore, we approximate the expectation of the strength of selection
 594 using a Taylor series:

$$\begin{aligned} \mathbb{E}[S(\varepsilon_c(t))] &= \left(\mathbb{E} \left[\sigma_z^2(\varepsilon_c(t)) \right] + \omega^2 \right)^{-1} - \frac{\text{Var}(\sigma_z^2)}{2\mathbb{E}[\sigma_z^2]^3} + O\left(\frac{\text{Var}(\sigma_z^2)^3}{\mathbb{E}[\sigma_z^2]^4} \right) \\ &\approx \left(\mathbb{E} \left[\sigma_z^2(\varepsilon_c(t)) \right] + \omega^2 \right)^{-1}. \end{aligned}$$

595 Expanding σ_z^2 using equation (1) of the main text and taking expectations, we get the approximate
 596 expected strength of selection S_δ , assuming $\delta \ll \sigma^2$, which we denote

$$S_\delta = \mathbb{E}[S(\varepsilon_c(t))] \approx \left(\sigma_a^2 + \sigma_b^2(\delta^2 + \sigma_c^2) + \sigma_e^2 + \omega^2 \right)^{-1}. \quad (\text{A.2})$$

597 Where we use the $\mathbb{E}[\varepsilon_c(t)^2] = \text{Var}[\varepsilon_c(t)] + \mathbb{E}[\varepsilon_c]^2$ and the mean environmental shift δ .

598 *Appendix A.2. Variance load*

599 The first term of equation (A.1) is the phenotypic variance load at time t

$$L_G(t) = 1/2 \log S(\varepsilon_c(t)) + 1/2 \log \omega^2.$$

600 Taking expectations, and using Taylor series:

$$\begin{aligned} \mathbb{E}[L_G] &= 1/2 \log \omega^2 + 1/2 \mathbb{E}[\log S(\varepsilon_c(t))] \\ &\approx 1/2 \log \omega^2 + 1/2 \log (\mathbb{E}[S(\varepsilon_c(t))]) - \frac{\text{Var}(\sigma_z^2)}{2\mathbb{E}[\sigma_z^2]^2} \\ &\approx 1/2 \log \omega^2 + 1/2 \log (\mathbb{E}[S(\varepsilon_c(t))]) \\ &\approx 1/2 \log \omega^2 + 1/2 \log S_\delta \end{aligned}$$

601 where the right hand side of the last line is the approximate expected variance load after using
602 $\mathbb{E}[S(\varepsilon_c(t))] \approx S_\delta$ from (A.2).

603 *Appendix A.3. Lag load*

604 The second term of equation (A.1) is the lag load at time t , $L_L(t)$. Here we show that in expectation,
605 this load has two components, a stochastic load and a shift load. To derive expressions for these, we
606 take the expectation of the entire second term:

$$\begin{aligned} \mathbb{E}[L_L(t)] &= \mathbb{E}\left[\frac{S(\varepsilon_c(t))}{2} x(t)^2\right], \\ &= \mathbb{E}\left[\frac{S(\varepsilon_c(t))}{2}\right] \mathbb{E}[x(t)^2] + \text{Cov}\left[\frac{S(\varepsilon_c(t))}{2}, x(t)^2\right], \end{aligned}$$

607 where we used the identity $\text{Cov}[ab] = \mathbb{E}[ab] - \mathbb{E}[a]\mathbb{E}[b]$. The covariance in the final line represents how
608 stochastic changes in environment (and optimum) that cause maladaptation also cause either larger or
609 smaller phenotypic variance, depending on the direction, due to our assumption that genetic variance
610 in plasticity increases with δ . Furthermore, under weak stabilizing selection, variance in z contributes
611 little to the strength of selection S . For both these reasons, we expect this covariance to be small.

612 If we neglect the covariance term and use the approximate variance load from Appendix A.2 (S_δ in
613 main text) the expectation is $\mathbb{E}[L_L(t)] \approx \frac{S_\delta}{2} \mathbb{E}[x(t)^2]$. Removing the expectation, we use this as to
614 approximate the dynamics of the lag load

$$L_L(t) = \frac{S_\delta}{2} x(t)^2.$$

615 *Appendix A.4. Full dynamics*

616 Bringing together the approximations developed above, we have an expression for the growth rate,
 617 where all components except the maladaptation are averaged over the fluctuations,

$$r(t) \approx r_{\max} + 1/2 \log(\omega^2 S_\delta) - \frac{S_\delta}{2} x(t)^2. \quad (\text{A.3})$$

618 From this, we can obtain both the average long-run growth rate, by taking an expectation to obtain
 619 $\bar{r}(t) \approx r_{\max} + 1/2 \log(\omega^2 S_\delta) - \frac{S_\delta}{2} (\bar{x}(t)^2 + \sigma_x^2(t))$ (because $\mathbb{E}[x^2] = \bar{x}^2 + \sigma_x^2$). This shows the lag load
 620 consists of two loads. The first, expected load from reduction in log mean fitness due to maladaptation
 621 of the mean trait relative to the mean optimum in the new environment, is “shift load” $-\frac{S_\delta}{2} \bar{x}(t)^2$.
 622 The second, expected load due to reduction in log mean fitness due to random fluctuations in the
 623 environment, is “stochastic load” $-\frac{S_\delta}{2} \sigma_x^2(t)$. We can also analyse the variance in trajectories of $r(t)$,
 624 and thus population growth because $\log N(t+1) = r(t) + \log N(t)$.

625 Both of our subsequent analyses require computing the dynamics of mean squared maladaptation $\bar{x}(t)^2$
 626 and the variance in maladaptation $\sigma_x^2(t)$.

627 **Appendix B. Dynamics of shift load depend on mean maladaptation $\bar{x}(t)^2$**

628 In this section, we derive the dynamics of the shift load $-\frac{S_\delta}{2} \bar{x}(t)^2$ under the approximation introduced
 629 by Lande [9] that separates adaptation into a fast Phase 1 and a slow Phase 2. We demonstrate that
 630 the population is approximately perfectly adapted in mean trait value by the end of Phase 1. We first
 631 write down the mean trait dynamics without the approximation, then describe the timescales of the
 632 two phase approximation, and derive approximate dynamics of the shift load owing to maladaptation in
 633 the mean trait.

634 *Appendix B.1. Mean trait*

635 Trait dynamics follow the standard equation $\Delta \mathbf{y} = \mathbf{G} \boldsymbol{\beta}$, where $\mathbf{y} = (\bar{a}, \bar{b})^T$, \mathbf{G} is the additive genetic
 636 variance-covariance matrix, and $\boldsymbol{\beta}$ is the selection gradient. The selection gradient on reaction norm
 637 height and slope obtained by taking the log-gradient of \bar{W} [from the equation for fitness above eq. (2)
 638 of main text; 9] is

$$\boldsymbol{\beta} = -S(\varepsilon_c(t)) \begin{pmatrix} \bar{a}(t) - A + \bar{b}(t)\varepsilon_c - B\varepsilon_s \\ (\bar{a}(t) - A + \bar{b}(t)\varepsilon_c - B\varepsilon_s) \varepsilon_c \end{pmatrix}. \quad (\text{B.1})$$

639 With a constant additive genetic variance-covariance matrix (\mathbf{G} matrix), the change per generation in
 640 $\bar{a}(t)$ and $\bar{b}(t)$ is given by

$$\Delta \begin{pmatrix} \bar{a}(t) \\ \bar{b}(t) \end{pmatrix} = \begin{pmatrix} \sigma_a^2 & 0 \\ 0 & \sigma_b^2 \end{pmatrix} \boldsymbol{\beta}.$$

641 In the new environment, the expectation of the change per generation conditional on \bar{a} and \bar{b} is

$$\begin{aligned} \Delta \begin{pmatrix} \mathbb{E}(\bar{a}(t)) \\ \mathbb{E}(\bar{b}(t)) \end{pmatrix} &= \mathbb{E}[\mathbf{G}\boldsymbol{\beta}] \\ &\approx -S_\delta \mathbf{G} \begin{pmatrix} \bar{a} - A + \bar{b}\delta - B\delta \\ \mathbb{E}[(\bar{a} - A)\varepsilon_c(t)] + \mathbb{E}[\bar{b}\varepsilon_c^2(t)] - B\mathbb{E}[\varepsilon_c\varepsilon_s] \end{pmatrix}, \end{aligned}$$

642 where the approximation comes from the treating $\mathbb{E}[S(\varepsilon_c(t))]$ as a constant. We assume no environmental
 643 tracking by phenotypic plasticity, i.e., $\text{Cov}[\bar{b}_t, \varepsilon_c(t)^2(t)] = 0$ so $\mathbb{E}[\bar{b}_t\varepsilon_c^2(t)] = \mathbb{E}[\bar{b}_t]\mathbb{E}[\varepsilon_c(t)^2(t)]$, or by reaction
 644 norm elevation, i.e., $\text{Cov}[\bar{a}_t, \varepsilon_c(t)] = 0$ so $\mathbb{E}[\bar{a}_t, \varepsilon_c(t)] = \mathbb{E}[\bar{a}_t]\mathbb{E}[\varepsilon_c(t)]$. Note that the tracking of the
 645 environment by the reaction norm elevation could be included, reducing the expected mean plasticity
 646 [28], but we neglect it here. However, we do allow for environmental tracking when computing the lag
 647 load (below). Then, using $\mathbb{E}[\varepsilon^2(t)] = \delta^2 + \sigma^2$ and $\mathbb{E}[\varepsilon_c(t)\varepsilon_s] = \delta^2 + \rho\sigma^2$, the expectation of the change is
 648 approximately

$$\mathbb{E} \left[\Delta \begin{pmatrix} \bar{a}(t) \\ \bar{b}(t) \end{pmatrix} \right] \approx -S_\delta \mathbf{G} \left[\begin{pmatrix} 1 & \delta \\ \delta & \delta^2 \end{pmatrix} \begin{pmatrix} \bar{a}(t) - A \\ \bar{b}(t) - B \end{pmatrix} + \begin{pmatrix} 0 \\ (\bar{b}(t) - \rho B)\sigma^2 \end{pmatrix} \right]. \quad (\text{B.2})$$

649 The approximation is exact if $\text{Cov}[\bar{b}_t, \varepsilon_c(t)^2(t)] = \text{Cov}[\bar{a}_t, \varepsilon_c] = 0$. Note that this differs from Lande [9],
 650 where this relation was treated as exact [28].

651 We solve for the explicit trait dynamics relative to the long-run equilibrium state [9]. Setting selection
 652 gradient $\boldsymbol{\beta}$ in equation (B.1) to zero, solve for long run trait values

$$\begin{pmatrix} \bar{a}_\infty \\ \bar{b}_\infty \end{pmatrix} = \begin{pmatrix} A + B\delta(1 - \rho\delta) \\ B\rho\delta \end{pmatrix} \quad (\text{B.3})$$

653 One can show, with some algebra [9], the one-generation change (B.2) is the product $-S_\delta \tilde{\mathbf{G}}\mathbf{z}(t)$, where
 654 $\mathbf{z}(t)$ is the difference between mean trait values and their long-run equilibrium values computed above
 655 and

$$\tilde{\mathbf{G}} = \begin{pmatrix} \sigma_a^2 & \sigma_a^2\delta \\ \sigma_b^2\delta & \sigma_b^2\delta^2 \left(1 + \frac{\sigma^2}{\delta^2}\right) \end{pmatrix}.$$

656 The expected dynamics can then be expressed in terms of the eigenvectors and eigenvalues of the matrix
 657 $\tilde{\mathbf{G}}$ [9, 16],

$$\mathbf{z}(t) = c_1 \mathbf{e}_1 (1 - S_\delta \lambda_1)^t + c_2 \mathbf{e}_2 (1 - S_\delta \lambda_2)^t, \quad (\text{B.4})$$

658 where \mathbf{e}_i and λ_i are eigenvectors and eigenvalues of $\tilde{\mathbf{G}}$ respectively and c_i terms are constants determined
 659 by initial conditions.

660 *Appendix B.2. Approximation for a large environmental shift*

661 As in earlier work, we consider the case where the shift in the mean environment is very large relative to
 662 background noise, $\frac{\sigma^2}{\delta^2} \ll 1$. Here, we initially write down the eigenvalues and eigenvectors of $\tilde{\mathbf{G}}$ to first
 663 order in this small term, but thereafter follow Chevin and Lande [16] in deriving approximate dynamics
 664 to leading order. To first order in $\frac{\sigma^2}{\delta^2}$, the eigenvalues are

$$\begin{pmatrix} \lambda_1 \\ \lambda_2 \end{pmatrix} = \begin{pmatrix} (\sigma_a^2 + \delta^2 \sigma_b^2) + \delta^2 \sigma_b^2 \frac{\sigma^2}{\delta^2} \phi \\ \sigma_a^2 \frac{\sigma^2}{\delta^2} \phi \end{pmatrix},$$

665 and the eigenvectors are

$$\mathbf{e}_1 = \begin{pmatrix} \delta(1 - \phi) \left(1 - \frac{\sigma^2}{\delta^2} \phi\right) \\ \phi \end{pmatrix}, \quad \mathbf{e}_2 = \begin{pmatrix} \delta \left(1 + \frac{\sigma^2}{\delta^2} \phi\right) \\ -1 \end{pmatrix}.$$

666 These match the calculations of [9] up to a constant of S_δ (equivalent to γ in Lande [9]).

667 Assuming the population has long evolved in an environment with predictability ρ , the initial trait
 668 values are $(\bar{a}_0, \bar{b}_0) = (A, \rho B)$. Using (B.3), the initial conditions in the re-centred trait x are

$$\mathbf{z}_0 = \begin{pmatrix} -B\delta(1 - \rho_\delta) \\ B(\rho - \rho_\delta) \end{pmatrix}$$

669 To leading order, the constants are

$$\begin{pmatrix} c1 \\ c2 \end{pmatrix} = \begin{pmatrix} -B(1 - \rho) \\ -B(\rho(1 - \phi) - \rho_\delta + \phi) \end{pmatrix}$$

670 *Appendix B.2.1. Timescales of phases 1 and 2*

671 If most phenotypic variation in the new environment is due to variance in plasticity, $\phi \approx 1$, and the shift
 672 in the mean environment is large (relative to background variability as in our approximation above),
 673 the trait change takes place in two phases that occur at very different timescales [9]. When selection is

674 weak, geometric terms in (B.4) can be replaced by exponential terms $e^{-tS_\delta\lambda_i}$, indicating the relative
675 timescales of change along the eigenvectors e_i are given by $t_i \approx \frac{1}{\lambda_i}$. The ratio $t_1/t_2 \approx \phi(1-\phi)\frac{\sigma_a^2}{\delta^2}$, and
676 when much of the additive genetic variation is due to variation in plasticity so $\phi \approx 1$, then $t_1/t_2 \approx \frac{\sigma_a^2}{\delta^2}$,
677 which is small in the approximate case we treat. Then, change along \mathbf{e}_1 occurs very fast relative to
678 change along \mathbf{e}_2 [9]. At the end of Phase 1, $e^{-tS_\delta\lambda_1} \approx 0$ while $e^{-tS_\delta\lambda_2} \approx 1$. Thus, the approximate state
679 of the system relative to its final state, i.e., (B.3), is $c_2\mathbf{e}_2$. The trait values, at the end of Phase 1 are,
680 to leading order,

$$\mathbb{E} \left[\begin{pmatrix} \bar{a}_{O(t_1)} \\ \bar{b}_{O(t_1)} \end{pmatrix} \right] \approx \begin{pmatrix} A + B\delta(1-\rho)(1-\phi) \\ B(\rho + \phi(1-\rho)) \end{pmatrix} \quad (\text{B.5})$$

681 The effect of the initial environment occurs through predictability ρ , which under our assumption that
682 the population is adapted initially also determines the initial mean plasticity $\bar{b}_0 = \rho B$. We see the
683 initial plasticity has a strong influence at the end of Phase 1 only if ϕ is small. When ϕ is large, the
684 plasticity at the end of Phase 1 is close to “perfect” i.e. $b_{O(t_1)} \approx B$. Note also that to first order, the
685 mean phenotype is perfectly adapted $\bar{z}_{O(t_1)} \approx A + B\delta$.

686 Where the extinction risk is calculated at half of the characteristic timescale of Phase 2, i.e., $t_{\text{bef}} = \frac{\phi\delta^2}{2\sigma_a^2\sigma_b^2}$

687 *Appendix B.2.2. Trait dynamics during Phase 1*

688 Throughout Phase 1, the term $(1 - S_\delta\lambda_2)^t \approx 1$, so the dynamics are given by

$$\mathbf{z}(t) = c_2\mathbf{e}_2 + c_1\mathbf{e}_1(1 - S_\delta\lambda_1)^t.$$

689 We again replace the geometric term with an exponential (valid for weak selection) and re-normalize.
690 To leading order, after some rearranging, the right hand side of the expected dynamics is

$$\mathbb{E} \left[\begin{pmatrix} \bar{a}(t) \\ \bar{b}(t) \end{pmatrix} \right] = (1 - e^{-tS_\delta\lambda_1}) B(1-\rho) \begin{pmatrix} \delta(1-\phi) \\ \phi \end{pmatrix} + \begin{pmatrix} A \\ B\rho \end{pmatrix}, \quad (\text{B.6})$$

691 which is analogous to the result of Chevin and Lande [Supporting Information, eq A6; 16]. As in that
692 paper, we compute the eigenvalue only to leading order in $\frac{\sigma_a^2}{\delta^2}$ so $\lambda_1 \approx \sigma_a^2 + \delta^2\sigma_b^2$ which is equivalent to
693 the expression $\frac{\sigma_a^2}{1-\phi}$ used in Chevin and Lande [16].

694 *Appendix B.2.3. Trait dynamics during Phase 2*

695 During Phase 2, the term $(1 - S_\delta\lambda_1)^t \approx 0$, so the dynamics are given by

$$\mathbf{z}(t) = c_2\mathbf{e}_2(1 - S_\delta\lambda_2)^t.$$

696 Then, using (B.3) and again replacing the geometric term with an exponential (valid for weak selection)
 697 and re-normalizing, the expected dynamics to leading order in $\frac{\sigma^2}{\delta^2}$ during Phase 2 are

$$\mathbb{E} \left[\begin{pmatrix} \bar{a}(t) \\ \bar{b}(t) \end{pmatrix} \right] = \begin{pmatrix} A + B\delta(1 - \rho_\delta) \\ B\rho_\delta \end{pmatrix} - B(\rho - \rho_\delta + \phi(1 - \rho)) \begin{pmatrix} \delta \\ -1 \end{pmatrix} e^{-tS\delta\sigma_a^2\frac{\sigma^2}{\delta^2}\phi}, \quad (\text{B.7})$$

698 where we have used $\lambda_2 \approx \sigma_a^2\frac{\sigma^2}{\delta^2}\phi$. Note that for $t = O(t_1)$, this exponential term equals 1 and this
 699 equation agrees with (B.5).

700 *Appendix B.3. Dynamics of expected maladaptation during Phase 1*

701 We derive the expected maladaptation of the mean trait during an initial phase of evolutionary rescue,
 702 focusing on a case where the size of the environmental shift is large and much of the additive genetic
 703 variance in the new environment owes to genetic variance in reaction norm slope. The shift load
 704 (computed in Appendix A) is $\frac{S\delta}{2}\bar{x}(t)^2$. After we compute the dynamics of the mean maladaptation
 705 $\bar{x}(t)^2$, we will have an approximation for dynamics of the shift load,

$$\begin{aligned} \bar{x}(t)^2 &= \mathbb{E}[x(t)]^2 = \left(\mathbb{E}[\bar{a}(t)] - A + \mathbb{E}[\bar{b}(t)\varepsilon_c(t)] - B\mathbb{E}[\varepsilon_s] \right)^2 \\ &\approx \left(\mathbb{E}[\bar{a}(t)] - A + \delta(\mathbb{E}[\bar{b}(t)] - B) \right)^2. \end{aligned}$$

706 The last equation comes from assuming the covariance between reaction norm slope and the cu-
 707 ing environment is small relative to the mean value of the new environment. Then, $\mathbb{E}[\bar{b}(t)\varepsilon_c(t)] \approx$
 708 $\mathbb{E}[\bar{b}(t)]\mathbb{E}[\varepsilon_c(t)] = \delta\mathbb{E}[\bar{b}(t)]$ in the new environment. This is reasonable when $\frac{\sigma^2}{\delta^2} \ll 1$. After using (B.6)
 709 and some algebra, we obtain

$$\bar{x}(t)^2 \approx B^2\delta^2(1 - \rho)^2 e^{-2tS\delta\frac{\sigma_a^2}{1-\phi}}. \quad (\text{B.8})$$

710 Where we use ϕ to represent the proportion of additive genetic variation in the new environment due to
 711 variation in plasticity,

$$\phi = \frac{\delta^2\sigma_b^2}{\sigma_a^2 + \delta^2\sigma_b^2}.$$

712 Equation (B.8) indicates the shift load goes to zero as t increases.

713 **Appendix C. Stochastic load: variance in maladaptation σ_x^2 at stationarity**

714 *Appendix C.1. Perceived environment with fixed plasticity*

715 A tactic from Michel *et al.* [35] aids in calculating the variance as a function of fixed plasticity. We define
 716 the perceived optimum $\psi(t)$ as the difference between the optimum and the mean trait after accounting

717 for the plastic response $\psi(t) = B\varepsilon_s(t) - \bar{b}^*\varepsilon_c(t)$ so that $x(t) = \bar{a}(t) - \psi(t)$. Then, the perceived variance
 718 in the optimum is

$$\sigma_\psi^2(\bar{b}^*, \rho_\delta) = \sigma^2(B^2 + \bar{b}^*(\bar{b}^* - 2B\rho_\delta)), \quad (\text{C.1})$$

719 and autocorrelation in the perceived optimum is

$$T_\psi(\bar{b}^*, \rho_\delta) = -\log \left[\rho_\delta^{1/\tau} \left(1 - \frac{B\bar{b}^*(\rho_\delta^{-1} - \rho_\delta)}{B^2 + \bar{b}^*(\bar{b}^* - 2B\rho_\delta)} \right) \right]^{-1} \quad (\text{C.2})$$

720 [35]. We can then express maladaptation in terms of the intercept and perceived environment as
 721 $x(t) = \bar{a}(t) - \psi(t)$.

722 *Appendix C.2. Variance at stationarity*

723 We derive an approximation for variance in maladaptation under stationarity, which we denote σ_x^2 .
 724 In practice, this means we solve for the effect of fluctuations on maladaptation after a long time, we
 725 assume the mean maladaptation is zero, and we also assume fixed mean plasticity \bar{b}^* . We are interested
 726 in finding an asymptotic expression for the variance of this term.

727 Assuming fixed plasticity, all change in the trait occurs through change in the reaction norm height,

$$\Delta \bar{z} = \Delta \bar{a}(t) = -S_\delta \sigma_a^2 x(t).$$

728 When selection is weak relative to genetic variance in reaction norm height, and the fluctuations in the
 729 perceived environment are not large, evolution can be approximated in continuous time [22, 35] as

$$\frac{dx}{dt} + S_\delta \sigma_a^2 x = -\frac{d\psi}{dt},$$

730 where $x = \bar{a}(t) - \psi$. For $t \gg t_1$ and constant genetic variance σ_a^2 , the solution to this differential
 731 equation is

$$\bar{a}(t) = S_\delta \sigma_a^2 \int_0^\infty \exp(-S_\delta \sigma_a^2 \tau) \psi(t - \tau) d\tau. \quad (\text{C.3})$$

732 What remains is to compute $\text{Var}[x(t)]$. Using our quasi-stationarity assumption, we need only compute
 733 $\mathbb{E}[x(t)^2] = -2\mathbb{E}[\bar{a}(t)\psi(t)] + \mathbb{E}[\bar{a}(t)^2] + \mathbb{E}[\psi(t)^2]$. The last of these expectations is simply the variance of
 734 the perceived environment σ_ψ^2 . The first and second expectations integrate over time (from eq. C.3),

$$\begin{aligned} -2\mathbb{E}[\bar{a}(t)\psi(t)] &= -2S_\delta \sigma_a^2 \int_0^\infty \exp(-S_\delta \sigma_a^2 \tau) \mathbb{E}[\psi(t)\psi(t - \tau)] d\tau \\ \mathbb{E}[\bar{a}(t)^2] &= S_\delta^2 \sigma_a^4 \int_0^\infty \int_0^\infty \exp(-S_\delta \sigma_a^2 (\tau_1 + \tau_2)) \mathbb{E}[\psi(t - \tau_1)\psi(t - \tau_2)] d\tau_1 d\tau_2. \end{aligned}$$

735 Because ψ is a linear combination of autoregressive Gaussian processes $\varepsilon_c(t)$ and ε_s , we can ex-
 736 press the expectations involving ψ in terms of autocovariance $\mathbb{E}[\psi(t), \psi(t - \tau)] = \sigma_\psi^2 \exp(-\tau/T_\psi)$ and
 737 $\mathbb{E}[\psi(t - \tau_1), \psi(t - \tau_2)] = \sigma_\psi^2 \exp(-|\tau_1 - \tau_2|/T_\psi)$. In both of these expressions, T_ψ is the characteristic
 738 autocorrelation time of the perceived environment ψ .

739 The first expectation is

$$\begin{aligned} -2\mathbb{E}[\bar{a}(t)\psi(t)] &= -2S_\delta\sigma_a^2\sigma_\psi^2 \int_0^\infty \exp(-\tau(S_\delta\sigma_a^2 + 1/T_\psi)) d\tau, \\ &= -2\frac{T_\psi S_\delta\sigma_a^2\sigma_\psi^2}{(T_\psi S_\delta\sigma_a^2 + 1)}. \end{aligned}$$

740 The second expectation involves an absolute value term, meaning the integral must be taken in two
 741 parts, and evaluates to

$$\begin{aligned} \mathbb{E}[\bar{a}(t)^2] &= S_\delta^2\sigma_a^4 \int_0^\infty \int_0^\infty \exp(-S_\delta\sigma_a^2(\tau_1 + \tau_2)) \sigma_\psi^2 \exp(-|\tau_1 - \tau_2|/T_\psi) d\tau_1 d\tau_2, \\ &= S_\delta\sigma_a^2\sigma_\psi^2 \frac{T_\psi}{(T_\psi S_\delta\sigma_a^2 + 1)} \end{aligned}$$

742 Combining these expressions,

$$\begin{aligned} \mathbb{E}[(\bar{a}(t) - \psi(t))^2] &= \sigma_\psi^2 \left(-2\frac{T_\psi S_\delta\sigma_a^2}{(T_\psi S_\delta\sigma_a^2 + 1)} + S_\delta\sigma_a^2 \frac{T_\psi}{(T_\psi S_\delta\sigma_a^2 + 1)} + 1 \right) \\ &= \frac{\sigma_\psi^2}{(T_\psi S_\delta\sigma_a^2 + 1)} (T_\psi S_\delta\sigma_a^2 + 1 - 2T_\psi S_\delta\sigma_a^2 + T_\psi S_\delta\sigma_a^2) \\ \sigma_x^2(\bar{b}^*, \delta, \rho_\delta) &:= \frac{\sigma_\psi^2}{(T_\psi S_\delta\sigma_a^2 + 1)}, \end{aligned}$$

743 where the last line defines the variance we sought to calculate. As our notation emphasizes, this load
 744 depends primarily on the level of plasticity \bar{b}^* and the size of the shift δ . Note that this formula matches
 745 Lande and Shannon [22].

746 *Appendix C.3. Quasi-stationary variance over Phase 1*

747 The variance in maladaptation σ_x^2 depends on variance $\sigma_\psi^2(\bar{b}^*, \rho_\delta)$ from eq. (C.1) and characteristic
 748 timescale $T_\psi(\bar{b}^*, \rho_\delta)$ from eq. (C.2) of perceived fluctuations in the perceived optimum (given autocorre-
 749 lation ρ_δ at timescale τ in the true optimum), as

$$\sigma_x^2(\bar{b}^*, \delta, \rho_\delta) = \frac{\sigma_\psi^2(\bar{b}^*, \rho_\delta)}{(S_\delta\sigma_a^2 T_\psi(\bar{b}^*, \rho_\delta) + 1)}. \quad (\text{C.4})$$

750 After a long time, on the timescale of Phase 1, t_1 , the mean maladaptation is zero, as shown in eq. (B.8),
 751 and the variance in maladaptation is stationary. At this point, as shown in Appendix B, plasticity is at
 752 its approximate maximum $b_{\max} = B(\rho + \phi(1 - \rho))$. It remains as this value for a long time (on the scale
 753 of Phase 1; although eventually decays to the predictability ρ_δ according to the dynamics in Appendix
 754 B.2.3) and so we evaluate (C.4) at b_{\max} to determine persistence in (3). Using the “quasi-stationary”
 755 approximation that fluctuations achieve stationarity while $\bar{b}^* = b_{\max}$, we evaluate $\sigma_x^2(b_{\max}, \delta, \rho_\delta)$.
 756 Note that we could also evaluate (C.4) at any time t during Phase 1,

$$\sigma_x^2(t) = \sigma_x^2(\bar{b}(t), \delta, \rho_\delta), \quad (\text{C.5})$$

757 by using dynamics for reaction norm slope $\bar{b}(t)$ from eq. (B.6). Doing so assumes for each change in \bar{b}
 758 over Phase 1 the stochastic variance in maladaptation achieves stationarity. No doubt this is inaccurate
 759 in some cases, but it is a tractable analytical approximation for the variance. Using this approximation
 760 over the parameter ranges we examine in this paper, the stochastic load does not change much with
 761 changes in plasticity (Figure S5). Accordingly, we use the simpler approximation above, and evaluate
 762 the variance at b_{\max} for all time.

763 Appendix D. Simulation

764 In simulation, we implement the autocorrelated environment as an autoregressive function with cor-
 765 relation κ on a timescale with $n = \text{ceiling}[\frac{1}{\tau}]$ time units in a generation. The process simulated
 766 is

$$x_i = \kappa x_{i-1} + \sqrt{1 - \kappa^2} \xi \sigma,$$

767 where ξ is a unit normal random variable. If x and ξ are independent (as generally assumed in
 768 autoregressive functions) and the process is stationary, it has variance σ^2 (and mean 0). Further, the
 769 covariance of observations one time unit apart is $\kappa\sigma^2$ and the correlation of such pairs of observations is
 770 κ . For observations n time units apart, the correlation becomes κ^n . Thus, using the n time steps per
 771 generation, the simulated process relates to the exponential autocovariance function given above as
 772 $\kappa^n = \rho^{1/\tau}$. Accordingly we set the correlation within simulations equal to that of the environmental
 773 predictability at timescale τ , i.e., $\kappa = \rho$.

774 **Appendix E. Alternative assumptions of reaction norm shape**

775 If, instead of assuming phenotypic variance in the reference environment is minimal, we assume the
 776 environment is shifted to an environment where the variance is minimal, then the additive genetic
 777 variance of the expressed trait $z(t)$ increases quadratically away from the novel environment $\varepsilon_c(t) = \delta$.
 778 Without the assumption that variance is minimized in the reference environment, the additive genetic
 779 covariance between a and b is non-zero in the reference environment [9]. From that paper, the full form
 780 of (1b) is $\sigma_z^2(\varepsilon_c(t)) = \sigma_a^2 + 2\sigma_{ab}\varepsilon_c(t) + \sigma_b^2\varepsilon_c^2(t) + \sigma_e^2$, where σ_{ab} is the additive genetic covariance between
 781 reaction norm slope and variance in the reference environment. (With the assumption of variance
 782 minimized at $\varepsilon_c = 0$, $\sigma_{ab} = 0$, and the covariance in any other environment is $\text{Cov}(a, b) = \sigma_b^2\varepsilon_c$.) Then
 783 $\sigma_z^2(\varepsilon_c(t))$ is minimized in the environment $\varepsilon_c^* = -\sigma_{ab}/\sigma_b^2$ [9].

784 Thus, assuming minimal variance in the new environment implies $\sigma_{ab} = -\delta\sigma_b^2$. The mean of the
 785 expressed trait value $z(t)$ before selection is the same as in (1), but the variance differs, giving

$$\bar{z}(t) = \bar{a}(t) + \bar{b}(t)\varepsilon_c(t) \tag{E.1a}$$

$$\sigma_z^2(\varepsilon_c(t)) = \sigma_a^2 - 2\sigma_b^2\delta\varepsilon_c(t) + \sigma_b^2\varepsilon_c^2(t) + \sigma_e^2, \tag{E.1b}$$

786 which assumes the additive genetic variances are constant in time.

787 In this case, the expressed trait z and the slope b have covariance $\text{Cov}(z, b) = (\varepsilon_c(t) - \delta)\sigma_b^2$ and so, with
 788 $\varepsilon_c(t) \approx \delta$ there is approximately zero covariance between the trait and reaction norm slope, and so
 789 direct selection on the trait results in very weak selection on reaction norm slope.

790 Consequently, the transient increase in plasticity should not be expected without the assumed increase
 791 of genetic variance in novel environments. Given the uncertainty described by McGuigan and Sgro [12]
 792 concerning the effects of stress (i.e., novelty) on additive genetic variance, theory could usefully outline
 793 empirical possibilities. The derivation of (E.1) is just the beginning. It does show, however, that the
 794 theory presented in the main text is not completely general. No theory is unless it thoroughly considers
 795 the possible relationships between additive genetic variance and environmental shifts. In the main text,
 796 we analyse only one set—where many are possible—of assumptions on how plasticity, demography,
 797 and evolution interact during evolutionary rescue. However, this set of assumptions appears met by
 798 empirical reality in at least some cases (see main text, "Assumptions and Caveats").

799 **Appendix F. A small shift and large additive variance in plasticity σ_b^2**

800 We expect our approximation to perform best when a large proportion of additive variance in the novel
801 environment is due to variance plasticity (i.e., $\phi \approx 1$). This occurs in our model either when σ_b^2 (GxE)
802 is large in the reference environment, or when a large shift in the mean environment causes quadratic
803 increases in additive genetic variance (as $\delta^2\sigma_b^2$).

804 In the former case, the population has inherently high genetic variability in plasticity, and our assumptions
805 imply a relatively large changes in additive genetic variance for even small shifts in the mean environment.
806 In the latter case, increased additive genetic variance is driven by the novelty of the environment.

807 Simulations reveal that despite both cases increasing ϕ , the approximation does not perform equiva-
808 lently well. If the mean shift is small then the approximation for the threshold between decline and
809 persistence performs poorly as additive variance in plasticity increases ($\delta = 1.5$, Figure S4). In fact, the
810 approximation appears to perform better for lower values of ϕ .

811 **Appendix G. Stochastic House of Cards Approximation**

812 Figure S3 shows effects of genetic variance changing with population size according to a modified
813 Stochastic House of Cards (SHC) approximation: $\sigma_{SHC}(\sigma_g^2) = \sigma_g^2 / (1 + \frac{\omega^2 + \sigma_e^2}{\mu^2 N_e})$ and $N_e \approx 2R_0N / (2R_0 - 1)$.
814 Parameters and panels are as in Figure 2 with the additional parameter μ^2 , which is the variance
815 of the effect of new mutations, fixed at $\mu^2 = 0.005$. For the un-modified SHC the numerator, σ_g^2 , is
816 replaced by a term that includes the per-generation total mutation rate V_m and the strength of selection:
817 $2V_m(\omega^2 + \sigma_e^2)$ [see 23, who used α^2 instead of μ^2]. Thus, the modified version we use effectively assumes
818 that larger initial values of σ_a^2 and σ_b^2 reflect populations with larger mutation rates.

819 **Appendix H. Supplementary Figures**

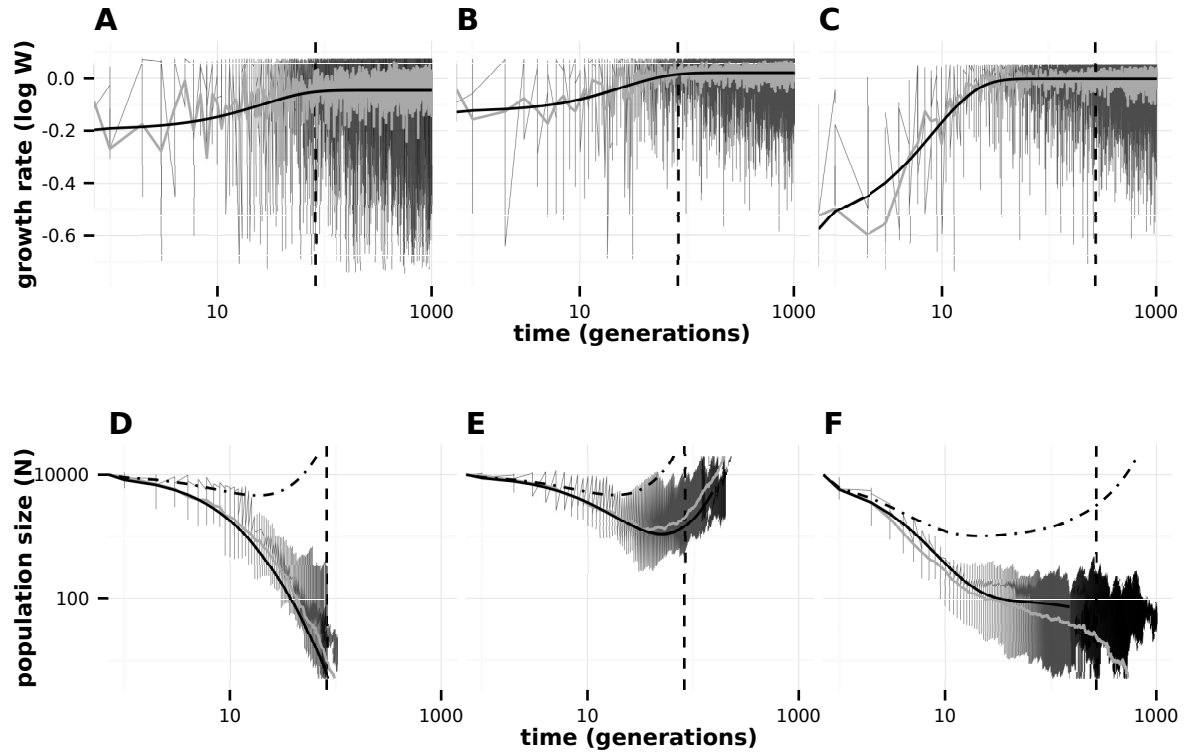


Figure S1: Dynamics of growth rate ($\log \bar{W}$, **A-C**), and population size ($\log N$, **D-F**) versus time (in generations, log scale) under evolutionary rescue for three scenarios of environmental shift δ and predictability ρ_δ following the shift: a modest shift and low predictability ($\delta = 2.5, \rho_\delta = 0.3$: **A,D**), a modest shift and high predictability ($\delta = 2.5, \rho_\delta = 0.7$: **B,E**), and a large shift and high predictability ($\delta = 5, \rho_\delta = 0.7$: **C,F**). Each panel shows 10 replicate simulations of 1500 generations (thin black lines), the mean of these simulations (thick grey line), and predicted trajectories of the mean (solid black line); also shown for comparison are predictions without amplifying effect of plasticity on stochastic fluctuations (dash-dot line). The dashed vertical lines indicate the time during Phase 1 at which we compute quasi-extinction before rescue (t_{bef} ; see Figure 1). Parameters: initial predictability $\rho = 0.5$, additive genetic variance in plasticity $\sigma_b^2 = 0.05$; other parameters as in Figure 2. Greater shift size implies larger increase of additive genetic variance in the new environment; for a modest shift (**A,B, D,E**) our model assumes additive genetic variance increases by a factor of 4, for a large shift, (**C,F**) the increase is by a factor of 14.

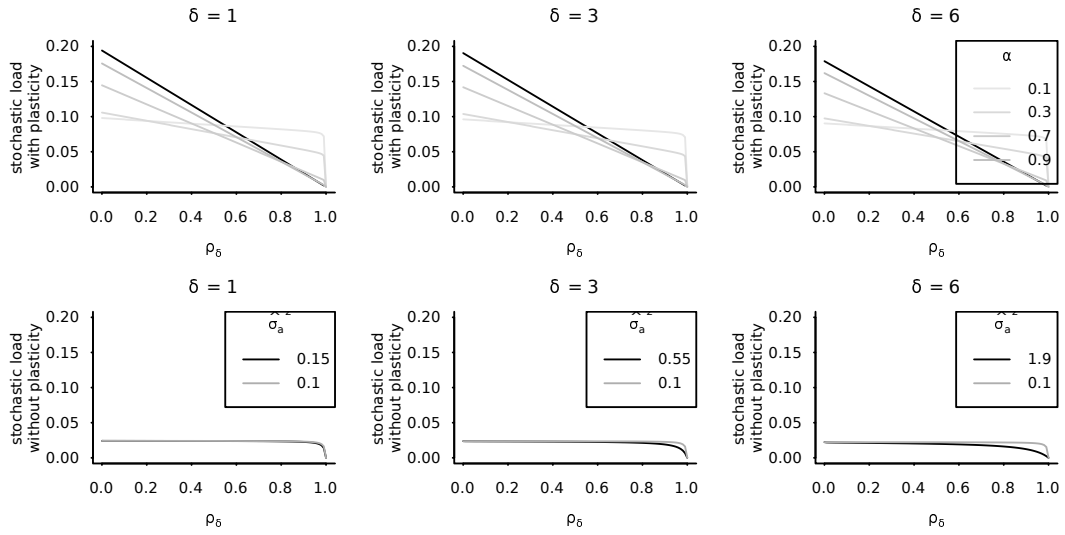


Figure S2: Top row: Stochastic load with plasticity plotted against ρ_δ for various values of relative plasticity α . Bottom row: Stochastic load without plasticity (i.e., load component for “positively auto-correlated fluctuations” from Table 1 of Lande and Shannon 1996) plotted against ρ_δ for equivalent values of total additive genetic variance. Specifically, the additive genetic variance in reaction norm elevation is adjusted to value $\hat{\sigma}_a^2$, set either to its initial value ($\hat{\sigma}_a^2 = \sigma_a^2$, grey line) or to the total additive genetic variance in the new environment with plasticity in the top row ($\hat{\sigma}_a^2 = \delta^2 \sigma_b^2 + \sigma_a^2$, black line). Also, note that relative plasticity α has no effect in the bottom row). Other parameters are $\sigma_b^2 = 0.05$, $\tilde{S}(\delta) = 0.0446429$, $B = 2$, $\sigma^2 = 1$, $\sigma_a^2 = 0.1$.

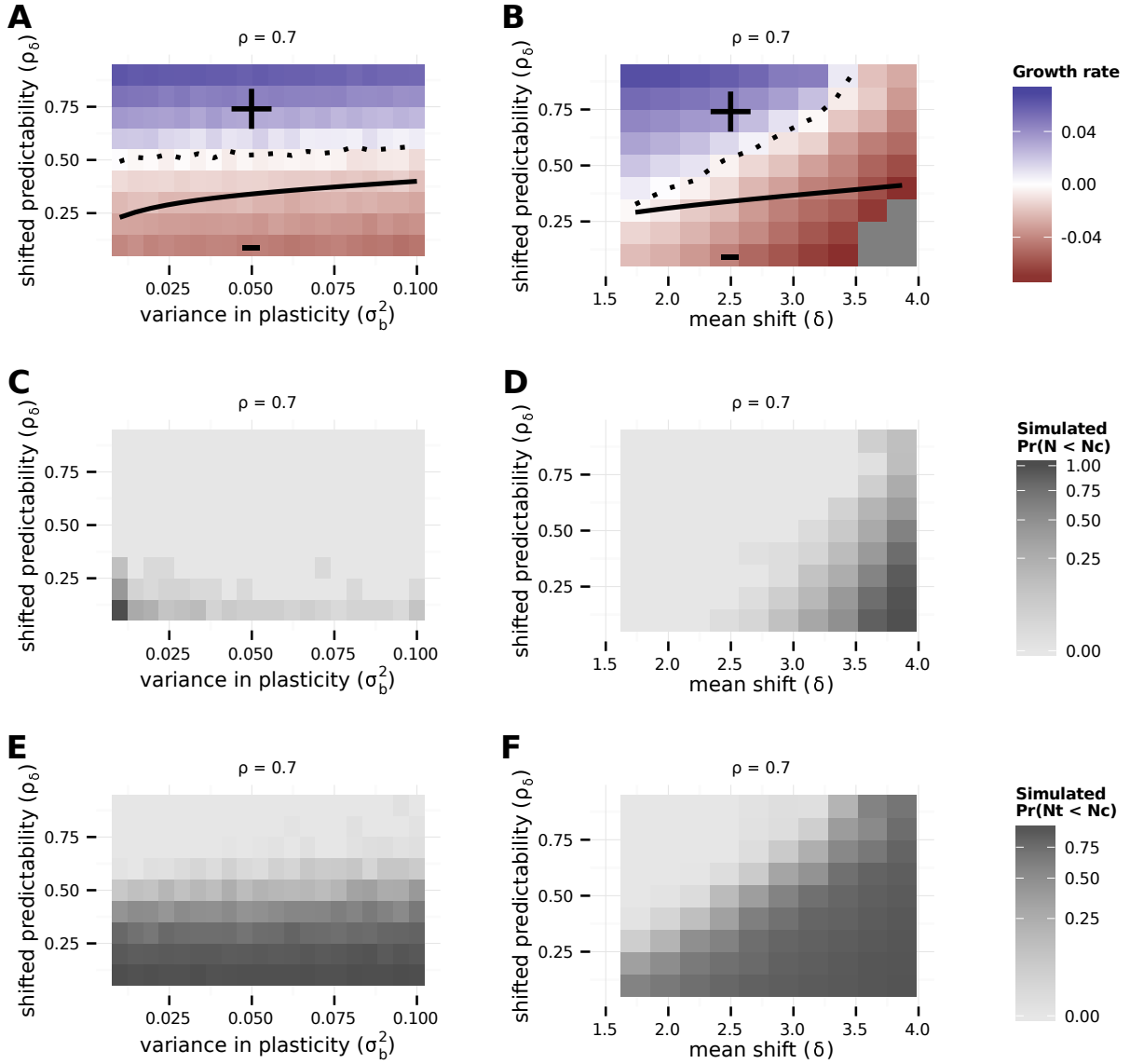


Figure S3: Figure 2 but with genetic variance changing with population size according to a modified Stochastic House of Cards (SHC) approximation: $\sigma_{SHC}(\sigma_g^2) = \sigma_g^2 / (1 + \frac{\omega^2 + \sigma_e^2}{\mu^2 N_e})$ and $N_e \approx 2R_0 N / (2R_0 - 1)$. Parameters and panels are as in Figure 2 with the additional parameter μ^2 , which is the variance of the effect of new mutations, fixed at $\mu^2 = 0.005$. For the un-modified SHC the numerator, σ_g^2 , is replaced by a term that includes the per-generation total mutation rate V_m and the strength of selection: $2V_m(\omega^2 + \sigma_e^2)$ [see 23, who used α^2 instead of μ^2]. Thus, the modified version we use effectively assumes that larger initial values of σ_a^2 and σ_b^2 reflect populations with larger mutation rates.

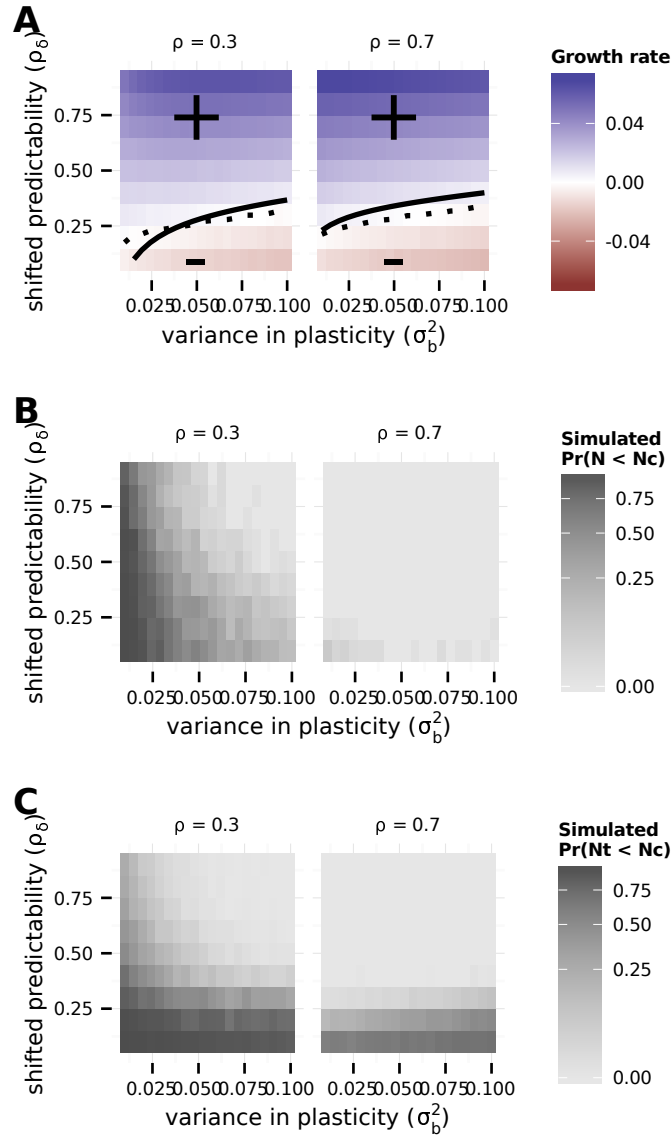


Figure S4: Potential for evolutionary rescue over a range of values for post-shift predictability ρ_δ versus genetic variance in plasticity the reference environment σ_b^2 (**A,B**). Within panels, columns show low ($\rho = 0.3$) and high ($\rho = 0.7$) initial predictability. **A** Growth rates at the end of rescue are computed from numerical simulations as the stochastic growth rate λ_s between t_{bef} and t_{aft} spanning Phase 1 and 2 (diverging heatmap: white 0, blue positive, and red negative). Black lines indicate the threshold between decline (-) and persistence (+) based on the analytical approximation ($\bar{r}_1 = 0$, eqn 3 ; solid line) and stochastic simulations ($\lambda_s = 0$, dotted black line). **B** Simulated probability of quasi-extinction before rescue. Quasi-extinction is defined at t_{bef} as illustrated in Figure 1. Shift size is set to $\delta = 2.5$ (so that additive variance increases by a factor of 4 in the new environment when $\sigma_b^2 = 0.05$). Other parameters: initial population size $N(0) = 10^4$, selection strength $\omega^2 = 20$, developmental delay $\tau = 0.2$, additive genetic $\sigma_a^2 = 0.1$ and environmental $\sigma_e^2 = 0.5$ variances, and maximum fitness $e^{r_{\text{max}}} = 1.1$.

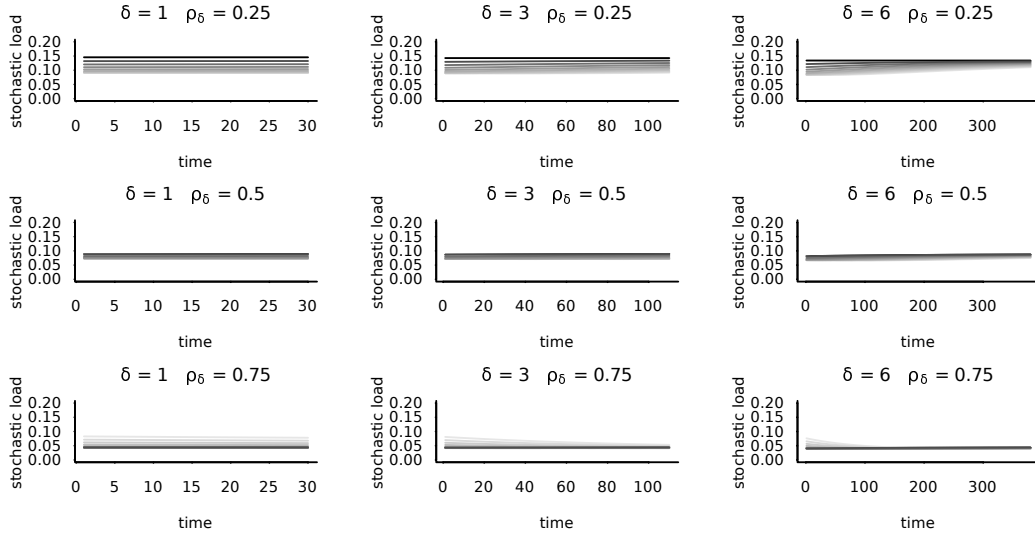


Figure S5: Quasi-stationary stochastic load plotted against time during Phase 1 (up to the characteristic timescale of Phase 2 t_2) for the same values of relative plasticity α as Figure S2. While changes in the magnitude of stochastic load over Phase 1 are not large, and in some cases not apparent, when the change reduces (or increases) the mismatch the stochastic load follows (e.g., bottom right or top right panel). Other parameters are $\sigma_b^2 = 0.05$, $\tilde{S}(\delta) = 0.0446429$, $B = 2$, $\sigma^2 = 1$, $\sigma_a^2 = 0.1$.

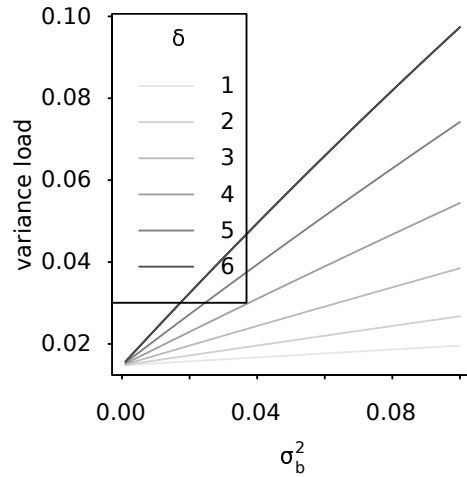


Figure S6: Variance load plotted against σ_b^2 for various values of δ . Other parameters are $B = 2$, $\sigma^2 = 1$, $\sigma_a^2 = 0.1$. Note predictability after shift ρ_δ does not affect variance load.